Gravitational Wave Imprints on Spontaneous Emission

Jerzy Paczos,[1,*] Navdeep Arya,[1,†] Sofia Qvarfort,[1,2,‡] Daniel Braun,[3,§] and Magdalena Zych[1,‖]
[1]Department of Physics, Stockholm University, SE-106 91 Stockholm, Sweden
[2]Nordita, KTH Royal Institute of Technology and Stockholm University, Hannes Alfvéns väg 12, SE-114 19 Stockholm, Sweden
[3]Institut für Theoretische Physik, Eberhard Karls Universität Tübingen, 72076 Tübingen, Germany

(Received 10 July 2025; revised 18 December 2025; accepted 2 February 2026; published 19 March 2026)

Despite growing interest, there is a scarcity of known predictions in the regime where both quantum and general relativistic effects become observable. Here, we investigate a combined atom-field system in a curved spacetime, with a specific focus on gravitational-wave backgrounds. We demonstrate that a plane gravitational wave alters spontaneous emission from a single atom, manifesting itself as a direction-dependent change in the emission spectrum. Although the total decay rate remains unchanged, implying that no information about the gravitational wave is stored in the atomic internal state alone, the wave leaves imprints on the evolution of the composite atom-field system. To quantify how well this effect can be measured, we analyze both the classical Fisher information associated with photon number measurements and the quantum Fisher information. Our analysis indicates that the effect could be measured in state-of-the-art cold-atom experiments and points to spontaneous emission as a potential probe of low-frequency gravitational waves.

DOI: 10.1103/1gtr-5c2f

Introduction—Currently testable general relativistic effects in Earth-based experiments comprise gravitational redshift tests [1,2] and gravitational wave (GW) detection [3,4]. In this context, GWs stand out as their measurements directly support the dynamical, curved spacetime predicted by general relativity. Since Einstein predicted GWs in 1916 [5] as ripples in the fabric of spacetime propagating at the speed of light, theoretical and experimental efforts have largely concentrated on understanding how these waves affect the motion of test masses [6–11]. Early analyses focused on the geodesic deviation induced by passing waves, which is at the heart of modern detection techniques and proposals, including ground-based laser interferometers [3,4], resonant bar detectors [8–11], pulsar timing arrays [12–14], space-based observatories [15], atom interferometers [16], levitated masses [17], and optical atomic clocks [18]. Despite their diversity, these approaches are unified by a common framework: the detection of GWs through their classical influence on the trajectories or separations of test masses.

Identifying testable general relativistic effects by means beyond classical test masses has been of increasing interest and importance in the foundations of physics. In this context, notable early steps toward exploring the effects of GWs involved studying their direct interaction with quantum systems. The interaction with a hydrogen atom was shown to induce small changes in its internal energy levels [19] and resonant quadrupole transitions [20]. These effects arise from the finite spatial extent of the atom and its quadrupole coupling to the GW amplitude and are potentially relevant for highly excited Rydberg atoms. The effect of GWs on other quantum systems has been studied in the context of particle production [21–26] and scattering [27], Rabi oscillations [28,29], field-mediated entanglement [30–32], and GW-induced superradiance in atomic arrays [33].

In this Letter, we investigate how a plane GW background affects spontaneous emission from a pointlike two-level atom. We show that a GW-induced periodic modulation of the quantum field interacting with the atom [27] gives rise to an angle-dependent correction to the emission spectrum. In the limit of large GW frequency, this leads to sidebands in the emission spectrum—a hallmark of periodically driven systems [34–38]. On the other hand, in the low GW frequency regime, the effect reduces to an angle-dependent frequency shift of the emitted photons. Moreover, the GW-induced correction exhibits a characteristic quadrupolar shape in the plane perpendicular to the GW propagation—a feature that may help distinguish this effect from other factors affecting

*Contact author: jerzy.paczos@fysik.su.se
†Contact author: navdeep.arya@fysik.su.se
‡Contact author: sofia.qvarfort@fysik.su.se
§Contact author: daniel.braun@uni-tuebingen.de
‖Contact author: magdalena.zych@fysik.su.se

Published by the American Physical Society under the terms of the Creative Commons Attribution 4.0 International license. Further distribution of this work must maintain attribution to the author(s) and the published article's title, journal citation, and DOI. Funded by Bibsam.

the spectrum. Interestingly, the total emission rate remains unchanged, indicating that no information about the GW is imprinted on the internal state of the atom. It is the quantum field—an extended system—that plays the central role by encoding information about the GW.

To assess the extractable information, we consider the estimation of the GW amplitude and analyze both the classical Fisher information associated with photon number measurements and the quantum Fisher information encoded in the atom-field state. We show that for a given GW frequency, there are optimal system-evolution times for which the quantum Cramér-Rao bound [39,40] can be saturated using photon number measurements. This is analogous to the optimal effective length in interferometric detectors [41]. Our analysis falls within the general framework for estimating spacetime parameters based on quantum measurements [42]. However, rather than focusing merely on the fields and working in the large-mean-field approximation (as in Ref. [42]), we consider the atom-field interaction in the weak-field regime (vacuum state), and our results do not follow from prior works. Finally, we estimate the minimal number of atoms required for GW detection based on the analysis of the classical and quantum Fisher information, and find that the requirements are not daunting. In particular, for shot-noise limited experiments, to reach the typically desired sensitivity [43,44] in the (sub) millihertz range, one would need at least 10^6–10^8 atoms (numbers that have already been achieved in experiments with cold atomic clouds [45–47]).

The method developed in this Letter can be applied to any spacetime metric on which quantum field theory has been developed [48–50]. This opens up the possibility of studying joint general relativistic and quantum effects in other spacetime geometries based on the effects in spontaneous emission proposed here. Throughout, we use natural units $\hbar = c = 1$.

Setup—Consider a simplified model of atom-light interaction, where the atom is treated as a pointlike two-level system with the ground state $|g\rangle$, the excited state $|e\rangle$, and the energy gap ω_0, and the light is modeled as a massless real scalar field $\hat{\phi}$. The field is assumed to couple linearly to the monopole moment of the atom $\hat{m}(\tau)$ through the (interaction picture) Hamiltonian

$$\hat{H}_I(\tau) = \varepsilon \hat{m}(\tau)\hat{\phi}[x(\tau)], \tag{1}$$

where τ is the proper time of the atom, $\varepsilon \ll 1$ is a small coupling constant, and $x(\tau) = [t(\tau), \boldsymbol{x}(\tau)]$ is the atomic trajectory. The monopole moment can be expressed in terms of raising and lowering operators $\hat{\sigma}_+ \equiv |e\rangle\langle g|$ and $\hat{\sigma}_- \equiv |g\rangle\langle e|$ as $\hat{m}(\tau) = e^{i\omega_0\tau}\hat{\sigma}_+ + e^{-i\omega_0\tau}\hat{\sigma}_-$. Given the spacetime metric and the complete set $\{u_{\boldsymbol{k}}, u^*_{\boldsymbol{k}}\}_{\boldsymbol{k}}$ of orthonormal solutions (modes) to the Klein-Gordon equation for the scalar field on that spacetime, we expand the field operator in the standard way,

$$\hat{\phi}[x(\tau)] = \int d^3\boldsymbol{k}\left[u_{\boldsymbol{k}}[x(\tau)]\hat{a}_{\boldsymbol{k}} + u^*_{\boldsymbol{k}}[x(\tau)]\hat{a}^\dagger_{\boldsymbol{k}}\right], \tag{2}$$

where the annihilation and creation operators $\hat{a}_{\boldsymbol{k}}$ and $\hat{a}^\dagger_{\boldsymbol{k}}$ satisfy $[\hat{a}_{\boldsymbol{k}}, \hat{a}^\dagger_{\boldsymbol{l}}] = \delta^{(3)}(\boldsymbol{k} - \boldsymbol{l})$ with other commutators vanishing. Information about the metric in the field expansion (2) is encoded in the modes $u_{\boldsymbol{k}}$.

The assumption of pointlike atoms and the use of the interaction Hamiltonian (1) exclude any direct coupling between the atoms and gravity. As a result, the small internal energy shifts [19] and resonant atom-GW interactions [20] (both potentially relevant for highly excited Rydberg atoms) are neglected in the present analysis. The effects described in this Letter result solely from the change of the field modes $u_{\boldsymbol{k}}$ due to gravity and are independent of the atom size (as long as it is much smaller than the GW wavelength and the atomic transition wavelength so that the pointlike approximation is valid).

The model constructed in Eq. (1) is known to capture the main features of the atom-light interaction under the assumption of interactions without exchange of angular momentum [51,52]. Note that GW effects on the total transition rate have been studied using this model, e.g., in [53,54], showing only quadratic dependence on the GW amplitude. In contrast, we show that the emission spectrum and directionality are affected in the first order in the GW amplitude and are, therefore, more relevant for potential experiments.

Spontaneous emission—We assume the initial atom-field state (at time τ_i) of the form $|\psi_0\rangle = |e\rangle \otimes |0\rangle$, where $|0\rangle$ is the field vacuum state defined by $\hat{a}_{\boldsymbol{k}}|0\rangle = 0$, and consider the state of the system at a later time τ_f,

$$|\psi(\tau_f, \tau_i)\rangle = \alpha(\tau_f, \tau_i)|e, 0\rangle + \int d^3\boldsymbol{k}\beta_{\boldsymbol{k}}(\tau_f, \tau_i)|g, 1_{\boldsymbol{k}}\rangle, \tag{3}$$

where $|1_{\boldsymbol{k}}\rangle \equiv \hat{a}^\dagger_{\boldsymbol{k}}|0\rangle$ is a single-photon state with the photon in mode $\boldsymbol{k}$. Up to the second order in ε, the coefficients α and $\beta_{\boldsymbol{k}}$ are given by

$$\begin{aligned}\alpha(\tau_f, \tau_i) &= 1 - \varepsilon^2 \int_{\tau_i}^{\tau_f} d\tau \int_{\tau_i}^{\tau} d\tau' e^{i\omega_0(\tau - \tau')} \times \\ &\quad \times \int d^3\boldsymbol{k} u_{\boldsymbol{k}}[x(\tau)]u^*_{\boldsymbol{k}}[x(\tau')], \\ \beta_{\boldsymbol{k}}(\tau_f, \tau_i) &= -i\varepsilon \int_{\tau_i}^{\tau_f} d\tau e^{-i\omega_0\tau} u^*_{\boldsymbol{k}}[x(\tau)].\end{aligned} \tag{4}$$

and to calculate them, we need to know the modes $u_{\boldsymbol{k}}$ and the trajectory $x(\tau)$. Equation (4) is valid for an arbitrary trajectory in a general spacetime in which quantum field theory is well defined [48–50], and therefore leads to testable predictions of quantum field theory in curved spacetimes.

As a specific example, consider the background metric corresponding to the plane, plus-polarized GW with amplitude $\mathcal{A}$ and frequency ω in the transverse-traceless gauge [41]

$$\begin{aligned} ds^2 = &-dt^2 + \{1 + \mathcal{A}\cos[\omega(t-z)]\}dx^2 \\ &+ \{1 - \mathcal{A}\cos[\omega(t-z)]\}dy^2 + dz^2. \end{aligned} \tag{5}$$

In this metric, trajectories with constant spatial coordinates (i.e., time independent) are geodesics, and $\tau = t$ is their proper time. Assume that the atom follows a geodesic with $x(t) = (t, \mathbf{0})$. The choice of x and y coordinates is arbitrary since the metric is homogeneous in the xy plane, while the selection of the z coordinate corresponds to the choice of the initial phase of the GW. With this choice of the atomic position, we can suppress the $\boldsymbol{x}$ dependence of the field operator by defining $\hat{\phi}(t) \equiv \hat{\phi}(t, \mathbf{0})$ and $u_{\boldsymbol{k}}(t) \equiv u_{\boldsymbol{k}}(t, \mathbf{0})$.

Given the metric (5), we can write the corresponding Klein-Gordon equation and construct the orthonormal solutions (see Ref. [27]) needed for the expansion (2). We introduce spherical coordinates in momentum space, $\boldsymbol{k} = k(\sin\theta\cos\varphi, \sin\theta\sin\varphi, \cos\theta)$, and a function $C_{\boldsymbol{k}} = \mathcal{A}(k/\omega)g(\theta,\varphi)$ with $g(\theta,\varphi) \equiv \cos^2(\theta/2)\cos(2\varphi)$. Then, the modes on the GW background are given by (see Supplemental Material [55])

$$u_{\boldsymbol{k}}(t) = \frac{1}{\sqrt{(2\pi)^3 2k}} e^{-i[kt - C_{\boldsymbol{k}}\sin(\omega t)]}, \tag{6}$$

corresponding to the flat-spacetime plane waves with periodically modulated phase.

For the metric (5) and the choice of mode solutions (6) the coefficient $\beta_{\boldsymbol{k}}$ from Eq. (4) is given by

$$\beta_{\boldsymbol{k}}(t_f, t_i) \propto \sum_{n=-\infty}^{\infty} J_n(C_{\boldsymbol{k}}) e^{-in\left(\phi_i + \frac{\omega T}{2}\right)} \operatorname{sinc}\left[\frac{(\delta_k - n\omega)T}{2}\right], \tag{7}$$

where we suppressed the overall factor for brevity (see Supplemental Material [55] for details). In Eq. (7) we denote by $J_n(C_{\boldsymbol{k}})$ the Bessel function of the first kind, $\phi_i \equiv \omega t_i$ is the initial phase of the GW, $\delta_k \equiv k - \omega_0$ is the atom-field-mode detuning, and $T \equiv t_f - t_i$ is the duration of the system evolution. Thus, the GW-induced modulation of the modes (6) gives rise to infinitely many sidebands with frequencies shifted by $n\omega$, and amplitudes $\propto J_n(C_{\boldsymbol{k}})$.

Given the coefficient $\beta_{\boldsymbol{k}}$, we can calculate the expected number of photons emitted into a specific mode, $\langle n_{\boldsymbol{k}}\rangle = |\beta_{\boldsymbol{k}}|^2$. The latter contains diagonal terms $\propto J_n^2(C_{\boldsymbol{k}})$ corresponding to the individual spectral components, and cross terms $\propto J_n(C_{\boldsymbol{k}})J_m(C_{\boldsymbol{k}})$ with $n \neq m$ representing interference between them. Up to the first order in $C_{\boldsymbol{k}}$ (and thus $\mathcal{A}$) the only terms that contribute are: the diagonal term $\propto J_0^2(C_{\boldsymbol{k}}) \approx 1$ (the carrier), and the interference terms between the carrier and the first sidebands $\propto J_0(C_{\boldsymbol{k}})J_{\pm1}(C_{\boldsymbol{k}}) \approx \pm C_{\boldsymbol{k}}/2$. We refer to the first one, being identical to the result in flat spacetime, as the flat-spacetime contribution, and denote it by $\langle \tilde{n}_{\boldsymbol{k}}\rangle$. The latter is subsequently called the GW correction and denoted by $\langle \delta n_{\boldsymbol{k}}\rangle$. They are given by (see Supplemental Material [55])

$$\begin{aligned} \langle \tilde{n}_{\boldsymbol{k}}\rangle &= \frac{\gamma_0 T^2}{8\pi^2\omega_0 k}\operatorname{sinc}^2(\delta_k T/2), \\ \langle \delta n_{\boldsymbol{k}}\rangle &= \frac{\gamma_0 T^2}{8\pi^2\omega_0 k} C_{\boldsymbol{k}}\cos(\phi_i + \omega T/2) f(\delta_k, T), \end{aligned} \tag{8}$$

where $\gamma_0 \equiv \varepsilon^2\omega_0/(2\pi)$ is the natural linewidth of the atomic transition, and $f(\delta_k, T) \equiv \operatorname{sinc}(\delta_k T/2)\{\operatorname{sinc}[(\delta_k - \omega)T/2] - \operatorname{sinc}[(\delta_k + \omega)T/2]\}$.

The function $f(\delta_k, T)$ determines the frequency dependence of the GW-induced correction $\langle \delta n_{\boldsymbol{k}}\rangle$. It is plotted in Fig. 1(a), which shows that GW induces positive and negative corrections on the sides of the carrier frequency ($\delta_k = 0$). The red dashed line in Fig. 1(a) marks the points corresponding to $\delta_k T = \pm 2\pi$, designating the width of the flat spacetime contribution $\langle \tilde{n}_{\boldsymbol{k}}\rangle$. For $\omega T \ll 2\pi$, the function reduces to two peaks, one on each side of $\delta_k = 0$ and both within the carrier range. This represents a small frequency shift of the carrier, $\Delta k/k = -\mathcal{A}\cos\phi_i g(\theta,\varphi)$, (see Supplemental Material [55]). On the other hand, for $\omega T \gtrsim 2\pi$ the correction $\langle \delta n_{\boldsymbol{k}}\rangle$ develops side peaks outside of the carrier (i.e., for $|\delta_k| > 2\pi/T$).

The angular dependence of the correction $\langle \delta n_{\boldsymbol{k}}\rangle$ is dictated by the factor $C_{\boldsymbol{k}} \propto g(\theta,\varphi)$ [see Fig. 1(b)]. It has a characteristic quadrupolar shape in the xy plane, reflecting the GW-induced deformation of space. Note that the correction is maximal along the direction of GW propagation and vanishes in the opposite direction. This directionality of the GW correction encodes information about the GW direction of propagation and its polarization, and is to be contrasted with the isotropy of the flat spacetime contribution.

Interestingly, the GW correction vanishes when integrated over the emitted photon's momentum, indicating that there is no net change in the total emission rate. Consequently, up to the first order in GW amplitude, no information about the GW is encoded in the atom's internal state—the atom acts only as a transducer of the information stored in the field.

The anticipated effect can be probed by performing a frequency- and angle-resolving photon number measurement and searching for an excess or deficit of photons with specific wave vectors. To retrieve the maximum information from the measurement, we need a spectral resolution Δk much smaller than the characteristic scale at which $\langle \delta n_{\boldsymbol{k}}\rangle$ varies significantly. The latter is given by the peak width of the function $f(\delta_k, T)$, which is $\sim T^{-1}$ [see Fig. 1(a)]. Since the spectral resolution is limited by the photon collection time $\Delta k \gtrsim T_{\mathrm{col}}^{-1}$, the ideal resolution requires $T_{\mathrm{col}} \gg T$. To

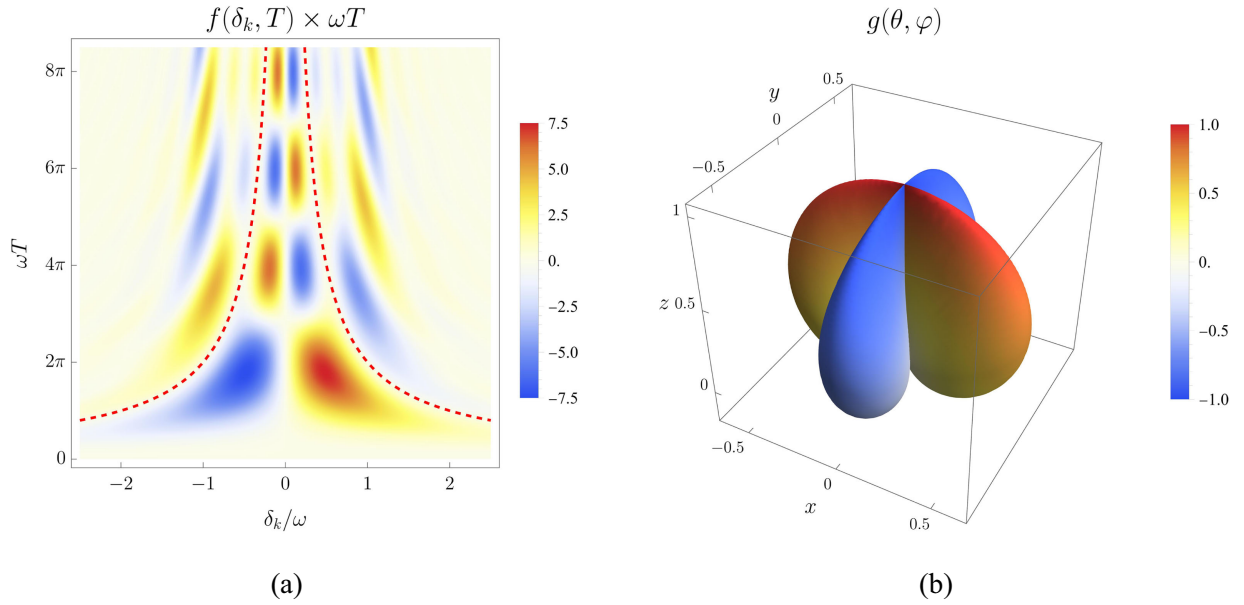


FIG. 1. Functions $f(\delta_k, T)$ and $g(\theta, \varphi)$ governing frequency and angular dependence of the GW correction to the photon emission. Their values are indicated by color, with blue and red corresponding to negative and positive values. From (a), it is apparent that the GW gives rise to positive and negative corrections on the sides of the carrier frequency ($\delta_k = 0$). The corrections are antisymmetric with respect to the carrier frequency. The red dashed lines in the plot correspond to $\delta_k T = \pm 2\pi$, designating the width of the flat spacetime contribution $\langle \tilde{n}_{\boldsymbol{k}} \rangle$. From the function $g(\theta, \varphi)$ in panel (b), it is apparent that the effect is maximal along the positive z direction (direction of GW propagation) and vanishes in the opposite direction. It exhibits a quadrupolar pattern in the xy plane with opposite signs along the x and y axes. The distance from the origin additionally highlights the absolute value of the function $g(\theta, \varphi)$ at given θ and φ.

ideally resolve the angular emission, we have to collect the photons from a small solid angle $\Delta\Omega \ll 1$ over which the function $g(\theta, \varphi)$ is approximately constant. Importantly, the ideal resolution is not necessary for detection. In fact, the predicted photon imbalance can be detected as long as the correction does not average out within the detection window $\Delta k \Delta\Omega$. In particular, for a generic evolution time T, the correction does not vanish when integrated over all positive (or negative) δ_k. Therefore, it is enough to detect an angle-dependent excess (or deficit) of photons with $\delta_k > 0$ with respect to those with $\delta_k < 0$ to retrieve some information about the GW.

The magnitude of the GW correction $\langle \delta n_{\boldsymbol{k}} \rangle$ is controlled by $C_{\boldsymbol{k}} \propto \mathcal{A}k/\omega$ [see Eq. (8)], in which the smallness of the GW amplitude $\mathcal{A}$ is (at least partially) balanced by the large factor k/ω. Specifically, for millihertz-frequency GWs and k in the visible range ($\sim 10^{14}$ Hz), the latter factor is $\sim 10^{17}$. The relevant GW sources in the millihertz frequency range are listed in Table I. Notably, for some of the strongest signals sourced by massive black-hole binaries, we have $C_{\boldsymbol{k}} \gtrsim 1$ and the expansion in powers of $C_{\boldsymbol{k}}$ leading to Eq. (8) is not accurate—one has to take into account other sidebands, which have non-negligible amplitudes. Here we focus on the (more usual) case in which $C_{\boldsymbol{k}} \ll 1$, but the effect is still greatly enhanced (as compared to the bare GW amplitude). Note that the same amplification mechanism [originating from the GW-induced phase modulation in Eq. (6)] is used in interferometric detectors [41], resulting in observable phase shifts.

Fisher information—To investigate how much information about the GW can be extracted from the system, consider the estimation of the GW amplitude $\mathcal{A}$ based on the (ideal-resolution) measurement of the observable $\hat{n}_{\boldsymbol{k}}$. The minimal achievable uncertainty $\delta\mathcal{A}$ of such an estimation is related to the classical Fisher information $\mathcal{I}_{\mathrm{C}}(\mathcal{A})$ associated with the measurement and the number M of independent repetitions of the measurement through [60,61] $\delta\mathcal{A} = 1/\sqrt{M\mathcal{I}_{\mathrm{C}}(\mathcal{A})}$. Treating $\langle n_{\boldsymbol{k}} \rangle$ as a probability density for a random variable $\boldsymbol{k}$ conditioned on the value of $\mathcal{A}$, we can calculate the classical Fisher information using the standard formula [62] $\mathcal{I}_{\mathrm{C}}(\mathcal{A}) = \int \mathrm{d}^3\boldsymbol{k} (\partial_{\mathcal{A}} \langle n_{\boldsymbol{k}} \rangle)^2 / \langle n_{\boldsymbol{k}} \rangle$. Up to the lowest (zeroth) order in $\mathcal{A}$ this gives (see Supplemental Material [55])

$$\mathcal{I}_{\mathrm{C}}(\mathcal{A}) = \frac{\bar{n}(T)}{3} \left(\frac{\omega_0}{\omega}\right)^2 \cos^2(\omega T/2 + \phi_i)[1 - \mathrm{sinc}(\omega T)], \tag{9}$$

where $\bar{n}(T) \equiv \gamma_0 T$ is the expected total number of photons emitted in time T. Note that Eq. (9) implicitly assumes shot-noise limited measurements—we do not include here the technical noise and systematics necessarily present in a real experiment.

TABLE I. Expected GW sources in the (sub)millihertz frequency range [59]: massive black-hole mergers (MBHMs), extreme mass-ratio inspirals (EMRI), and galactic binaries (GBs).

Source	Frequency	Amplitude
MBHMs	$\sim 10^{-4} - 10^{-1}$ Hz	$\lesssim 10^{-16}$
EMRIs	$\sim 10^{-3} - 10^{-1}$ Hz	$\lesssim 10^{-18}$
GBs	$\sim 10^{-4} - 10^{-2}$ Hz	$\lesssim 10^{-18}$

The ultimate upper bound on the classical Fisher information is set by the quantum Fisher information $\mathcal{I}_{\mathrm{C}}(\mathcal{A}) \leq \mathcal{I}_{\mathrm{Q}}(\mathcal{A})$. The latter quantity is measurement-independent and represents the maximum amount of information (about a given parameter) that can be extracted from the quantum state under an optimal measurement strategy [39]. For the joint atom-field state $|\psi(t_f, t_i)\rangle$, the quantum Fisher information associated with the estimation of $\mathcal{A}$ is given by $\mathcal{I}_{\mathrm{Q}}(\mathcal{A}) = 4(\langle \partial_{\mathcal{A}}\psi(t_f,t_i)|\partial_{\mathcal{A}}\psi(t_f,t_i)\rangle - |\langle \psi(t_f,t_i)|\partial_{\mathcal{A}}\psi(t_f,t_i)\rangle|^2)$ and reads (see Supplemental Material [55])

$$\mathcal{I}_{\mathrm{Q}}(\mathcal{A}) = \frac{\bar{n}(T)}{3}\left(\frac{\omega_0}{\omega}\right)^2 [1 - \cos(\omega T + 2\phi_i)\mathrm{sinc}(\omega T)]. \tag{10}$$

Note that at times $T_m = 2(m\pi - \phi_i)/\omega$ with $m \in \mathbb{N}$, the classical and quantum Fisher information coincide, and thus, at those specific times, the photon-number measurement provides maximum information about $\mathcal{A}$. For this reason, we call the times T_m the optimal evolution times.

The optimal evolution times are analogous to the optimal effective arm lengths (effectively determining the GW-light interaction time) in interferometric detectors [41]. In interferometers, this effective length is practically limited by the physical length of the arms and the quality of the mirrors used to enhance it. In contrast, in the present scheme, the evolution time is ultimately constrained by the lifetime of the atomic transition under consideration. Notably, for the narrow-linewidth transitions used in optical atomic clocks [63], such as the $^1S_0 \leftrightarrow {}^3P_0$ transition in ^{87}Sr with a lifetime of approximately 100 s [64–67], the available interaction time is generally much longer than that achievable in ground-based interferometers (typically $\sim 10^{-3}$ seconds for LIGO and Virgo). This suggests that the predicted modifications to the atomic emission spectrum could be advantageous for detecting GWs at lower frequencies, which are beyond the reach of current ground-based interferometers.

Discussion—For the GW to be (in principle) detectable through this mechanism, the measurement-specific variance must be $\delta\mathcal{A} \lesssim \mathcal{A}$, which means $\mathcal{A} \gtrsim 1/\sqrt{M\mathcal{I}_{\mathrm{C}}(\mathcal{A})}$. This puts a constraint on the minimal number M of repetitions of the experiment needed for GW detection, namely $M \gtrsim (\mathcal{A}^2\mathcal{I}_{\mathrm{C}}(\mathcal{A}))^{-1}$. In experiments with many independent atoms, we can think of M as the number of atoms used. Since Eq. (9) has been derived using perturbation theory, it gives reliable predictions only for times much smaller than the lifetime of the excited state, $\gamma_0 T \ll 1$. Therefore, in Supplemental Material [55] we outline the spontaneous emission description using Weisskopf-Wigner theory [68,69], which is valid for times comparable to and larger than the excited state lifetime, $\gamma_0 T \gtrsim 1$. In this long-evolution-time limit, the classical Fisher information scales with the square of the quality factor of the transition $Q = \omega_0/\gamma_0$, and in the limit of low GW frequency, $\omega \ll \gamma_0$, it reduces to $\mathcal{I}_{\mathrm{C}}(\mathcal{A}) = (Q^2/3)\cos^2\phi_i$. Thus, the minimal number of atoms required for the detection of such GWs is $M \sim (Q\mathcal{A})^{-2}$. Note that the same scaling can be obtained from Eq. (9) by setting the evolution time to $T = 1/\gamma_0$ (lifetime of the excited state) and considering the low-frequency limit, $\omega T \ll 1$.

The strontium-87 $^1S_0 \leftrightarrow {}^3P_0$ transition used in the most precise optical atomic clocks to date [1,2] has the natural linewidth $\gamma_0/(2\pi) \approx 1.35$ mHz [65], and the quality factor $Q \approx 3.18 \times 10^{17}$. Therefore, to be able to resolve the GW signal in the submillihertz frequency range with amplitude $\mathcal{A} \sim 10^{-20} - 10^{-21}$ (corresponding to the expected sensitivity of LISA [43,44]), one would have to collect the emitted photons from at least $M \sim 10^6 - 10^8$ atoms. For example, assuming a gravitational wave with amplitude $\mathcal{A} = 10^{-21}$ and frequency $\omega/(2\pi) = 0.1$ mHz, one would need at least $M \approx 3.15 \times 10^7$ atoms according to our estimates. These numbers would be even lower for the nuclear transition in ^{229}Th, with a quality factor $Q \sim 10^{19} - 10^{20}$ [70,71], and GWs with frequencies $\omega \lesssim 10^{-5}$ Hz (the latter being the linewidth of the transition). Note that these are just rough estimates assuming shot-noise-limited measurements. To assess the practical feasibility of GW detection using the scheme proposed in this Letter, a thorough analysis of additional noise sources is essential. These include standard sources encountered in high-precision fluorescence spectroscopy, such as readout noise, environmental disturbances, and trap-specific noise in the case of confined atoms.

Conclusion—We have shown that GWs modulate the quantum field interacting with atoms, leading to distinctive, angle-dependent features in the spontaneous emission spectrum—manifesting as frequency shifts or sidebands. This reveals a new and fundamental imprint of spacetime dynamics within quantum field theory on curved backgrounds, with promising experimental implications. Our results establish a concrete framework for exploring gravitational effects in atom–light interactions, opening new avenues for quantum probes of gravity. Beyond their foundational significance, these findings motivate the development of detection schemes that harness signatures of GWs in atomic spectra, together with detailed studies of realistic noise and sensitivity in future experiments.

Acknowledgments—We thank Igor Pikovski, Hendrik Ulbricht, T. Rick Perche, Rafał Demkowicz-Dobrzański, and Dhruva Ganapathy for helpful discussions and useful comments. J. P., N. A., and M. Z. acknowledge the Knut and Alice Wallenberg Foundation through a Wallenberg Academy Fellowship No. 2021.0119. S. Q. is funded in part by the Wallenberg Initiative on Networks and Quantum Information (WINQ) and in part by the Marie Skłodowska–Curie Action IF programme *Nonlinear optomechanics for verification, utility, and sensing* (NOVUS)—Grant No. 101027183. Nordita is funded in part by NordForsk. D. B. acknowledges support by the EU EIC Pathfinder Project No. QuCoM (101046973).

Data availability—The data that support the findings of this article are not publicly available. The data are available from the authors upon reasonable request.

[1] T. Bothwell, C. J. Kennedy, A. Aeppli, D. Kedar, J. M. Robinson, E. Oelker, A. Staron, and J. Ye, Resolving the gravitational redshift across a millimetre-scale atomic sample, Nature (London) **602**, 420 (2022).
[2] X. Zheng, J. Dolde, V. Lochab, B. N. Merriman, H. Li, and S. Kolkowitz, Differential clock comparisons with a multiplexed optical lattice clock, Nature (London) **602**, 425 (2022).
[3] F. Acernese *et al.*, Advanced Virgo: A second-generation interferometric gravitational wave detector, Classical Quantum Gravity **32**, 024001 (2014).
[4] LIGO Scientific Collaboration *et al.*, Advanced LIGO, Classical Quantum Gravity **32**, 074001 (2015).
[5] A. Einstein, Näherungsweise Integration der Feldgleichungen der Gravitation, Sitzungsber. K. Preuß. Akad. Wiss. **1916**, 688.
[6] F. A. E. Pirani, On the physical significance of the Riemann tensor, Acta Phys. Pol. **15**, 389 (1956).
[7] H. Bondi, F. A. E. Pirani, and I. Robinson, Gravitational waves in general relativity III: Exact plane waves, Proc. R. Soc. A **251**, 519 (1959).
[8] J. Weber, Detection and generation of gravitational waves, Phys. Rev. **117**, 306 (1960).
[9] J. Weber, Observation of the thermal fluctuations of a gravitational-wave detector, Phys. Rev. Lett. **17**, 1228 (1966).
[10] J. Weber, Gravitational radiation, Phys. Rev. Lett. **18**, 498 (1967).
[11] J. Weber, Gravitational-wave-detector events, Phys. Rev. Lett. **20**, 1307 (1968).
[12] M. V. Sazhin, Opportunities for detecting ultralong gravitational waves, Sov. Astron. **22**, 36 (1978).
[13] S. Detweiler, Pulsar timing measurements and the search for gravitational waves, Astrophys. J. **234**, 1100 (1979).
[14] R. Hellings and G. Downs, Upper limits on the isotropic gravitational radiation background from pulsar timing analysis, Astrophys. J. Lett. **265**, L39 (1983).
[15] J. W. Armstrong, F. B. Estabrook, and M. Tinto, Time-delay interferometry for space-based gravitational wave searches, Astrophys. J. **527**, 814 (1999).
[16] S. Dimopoulos, P. W. Graham, J. M. Hogan, M. A. Kasevich, and S. Rajendran, Atomic gravitational wave interferometric sensor, Phys. Rev. D **78**, 122002 (2008).
[17] A. Arvanitaki and A. A. Geraci, Detecting high-frequency gravitational waves with optically levitated sensors, Phys. Rev. Lett. **110**, 071105 (2013).
[18] S. Kolkowitz, I. Pikovski, N. Langellier, M. D. Lukin, R. L. Walsworth, and J. Ye, Gravitational wave detection with optical lattice atomic clocks, Phys. Rev. D **94**, 124043 (2016).
[19] T. Leen, L. Parker, and L. O. Pimentel, Remote quantum mechanical detection of gravitational radiation, Gen. Relativ. Gravit. **15**, 761 (1983).
[20] U. Fischer, Transition probabilities for a Rydberg atom in the field of a gravitational wave, Classical Quantum Gravity **11**, 463 (1994).
[21] G. Gibbons, Quantized fields propagating in plane-wave spacetimes, Commun. Math. Phys. **45**, 191 (1975).
[22] S. Deser, Plane waves do not polarize the vacuum, J. Phys. A **8**, 1972 (1975).
[23] F. Sorge, Do gravitational waves create particles?, Classical Quantum Gravity **17**, 4655 (2000).
[24] C. Sabín, D. E. Bruschi, M. Ahmadi, and I. Fuentes, Phonon creation by gravitational waves, New J. Phys. **16**, 085003 (2014).
[25] P. Jones, P. McDougall, and D. Singleton, Particle production in a gravitational wave background, Phys. Rev. D **95**, 065010 (2017).
[26] F. Gray, D. Kubizňák, A. May, and R. B. Mann, Quantum imprints of gravitational shockwaves, J. High Energy Phys. 11 (2021) 054.
[27] J. Garriga and E. Verdaguer, Scattering of quantum particles by gravitational plane waves, Phys. Rev. D **43**, 391 (1991).
[28] S. Siparov, A two-level atom in the field of a gravitational wave—On the possibility of parametric resonance, Astron. Astrophys. **416**, 815 (2004).
[29] F. Sorge, Jaynes–Cummings model in a weak gravitational wave background, Classical Quantum Gravity **41**, 015028 (2023).
[30] Q. Xu, S. Ali Ahmad, and A. R. H. Smith, Gravitational waves affect vacuum entanglement, Phys. Rev. D **102**, 065019 (2020).
[31] S. Barman, I. Chakraborty, and S. Mukherjee, Entanglement harvesting for different gravitational wave burst profiles with and without memory, J. High Energy Phys. 09 (2023) 180.
[32] S. Barman, I. Chakraborty, and S. Mukherjee, Signatures of gravitational wave memory in the radiative process of entangled quantum probes, Phys. Rev. D **111**, 025021 (2025).
[33] N. Arya and M. Zych, Selective amplification of a gravitational wave signal using an atomic array, arXiv:2408.12436.
[34] S. H. Autler and C. H. Townes, Stark effect in rapidly varying fields, Phys. Rev. **100**, 703 (1955).
[35] B. R. Mollow, Power spectrum of light scattered by two-level systems, Phys. Rev. **188**, 1969 (1969).
[36] R. E. Grove, F. Y. Wu, and S. Ezekiel, Measurement of the spectrum of resonance fluorescence from a two-level atom in an intense monochromatic field, Phys. Rev. A **15**, 227 (1977).

[37] A. Boca, R. Miller, K. M. Birnbaum, A. D. Boozer, J. McKeever, and H. J. Kimble, Observation of the vacuum Rabi spectrum for one trapped atom, Phys. Rev. Lett. **93**, 233603 (2004).
[38] P. Maunz, T. Puppe, I. Schuster, N. Syassen, P. W. H. Pinkse, and G. Rempe, Normal-mode spectroscopy of a single-bound-atom–cavity system, Phys. Rev. Lett. **94**, 033002 (2005).
[39] S. L. Braunstein and C. M. Caves, Statistical distance and the geometry of quantum states, Phys. Rev. Lett. **72**, 3439 (1994).
[40] S. L. Braunstein, C. M. Caves, and G. Milburn, Generalized uncertainty relations: Theory, examples, and Lorentz invariance, Ann. Phys. (N.Y.) **247**, 135 (1996).
[41] M. Maggiore, *Gravitational Waves: Volume 1: Theory and Experiments* (Oxford University Press, Oxford, 2007).
[42] T. G. Downes, J. R. van Meter, E. Knill, G. J. Milburn, and C. M. Caves, Quantum estimation of parameters of classical spacetimes, Phys. Rev. D **96**, 105004 (2017).
[43] T. Robson, N. J. Cornish, and C. Liu, The construction and use of LISA sensitivity curves, Classical Quantum Gravity **36**, 105011 (2019).
[44] S. Babak, M. Hewitson, and A. Petiteau, LISA sensitivity and SNR calculations, Technical Note LISA-LCST-SGS-TN-001, LISA Consortium, 2021, [arXiv:2108.01167].
[45] G. Labeyrie, F. de Tomasi, J.-C. Bernard, C. A. Müller, C. Miniatura, and R. Kaiser, Coherent backscattering of light by cold atoms, Phys. Rev. Lett. **83**, 5266 (1999).
[46] W. Guerin, M. O. Araújo, and R. Kaiser, Subradiance in a large cloud of cold atoms, Phys. Rev. Lett. **116**, 083601 (2016).
[47] S. V. Kashanian, A. Eloy, W. Guerin, M. Lintz, M. Fouché, and R. Kaiser, Noise spectroscopy with large clouds of cold atoms, Phys. Rev. A **94**, 043622 (2016).
[48] N. D. Birrell and P. C. W. Davies, *Quantum Fields in Curved Space*, Cambridge Monographs on Mathematical Physics (Cambridge University Press, Cambridge, England, 1982).
[49] R. M. Wald, *Quantum Field Theory in Curved Spacetime and Black Hole Thermodynamics*, Chicago Lectures in Physics (University of Chicago Press, Chicago, 1994).
[50] V. Mukhanov and S. Winitzki, *Introduction to Quantum Effects in Gravity*, Cambridge Monographs on Mathematical Physics (Cambridge University Press, Cambridge, England, 2007).
[51] E. Martín-Martínez, M. Montero, and M. del Rey, Wavepacket detection with the Unruh-DeWitt model, Phys. Rev. D **87**, 064038 (2013).
[52] A. M. Alhambra, A. Kempf, and E. Martín-Martínez, Casimir forces on atoms in optical cavities, Phys. Rev. A **89**, 033835 (2014).
[53] B.-H. Chen and D.-W. Chiou, Response of the Unruh-DeWitt detector in a gravitational wave background, Phys. Rev. D **105**, 024053 (2022).
[54] T. Prokopec, Gravitational wave signals in an Unruh–DeWitt detector, Classical Quantum Gravity **40**, 035007 (2023).
[55] See Supplemental Material at http://link.aps.org/supplemental/10.1103/1gtr-5c2f for details on the orthonormal modes, perturbative system evolution, low-frequency regime, Fisher-information calculations, and the Weisskopf-Wigner approach. Supplemental Material includes Refs. [56–58].
[56] H. A. Bethe, The electromagnetic shift of energy levels, Phys. Rev. **72**, 339 (1947).
[57] R. Loudon, *The Quantum Theory of Light*, 3rd ed. (Oxford University Press, New York, 2000).
[58] C. C. Gerry and P. L. Knight, *Introductory Quantum Optics* (Cambridge University Press, Cambridge, England, 2005).
[59] J. R. Gair, M. Vallisneri, S. L. Larson, and J. G. Baker, Testing general relativity with low-frequency, space-based gravitational-wave detectors, Living Rev. Relativity **16**, 7 (2013).
[60] H. Cramér, *Mathematical Methods of Statistics* (Princeton University Press, Princeton, NJ, 1946).
[61] C. R. Rao, Information and the accuracy attainable in the estimation of statistical parameters, Bull. Calcutta Math. Soc. **37**, 81 (1945).
[62] R. A. Fisher, On the mathematical foundations of theoretical statistics, Phil. Trans. R. Soc. A **222**, 309 (1922).
[63] A. D. Ludlow, M. M. Boyd, J. Ye, E. Peik, and P. O. Schmidt, Optical atomic clocks, Rev. Mod. Phys. **87**, 637 (2015).
[64] S. Dörscher, R. Schwarz, A. Al-Masoudi, S. Falke, U. Sterr, and C. Lisdat, Lattice-induced photon scattering in an optical lattice clock, Phys. Rev. A **97**, 063419 (2018).
[65] J. A. Muniz, D. J. Young, J. R. K. Cline, and J. K. Thompson, Cavity-QED measurements of the ^{87}Sr millihertz optical clock transition and determination of its natural linewidth, Phys. Rev. Res. **3**, 023152 (2021).
[66] X.-T. Lu, F. Guo, Y.-Y. Liu, J.-J. Xia, G.-D. Zhao, Y.-X. Chen, Y.-B. Wang, B.-Q. Lu, and H. Chang, Determining the lifetime of the $5s5p\,^3P_0^o$ metastable state in ^{87}Sr from the electric dipole matrix element, Phys. Rev. Appl. **21**, 024042 (2024).
[67] J. Dolde, D. Ganapathy, X. Zheng, S. Ma, K. Beloy, and S. Kolkowitz, Direct measurement of the $^3P_0$ clock state natural lifetime in ^{87}Sr, Phys. Rev. A **112**, 023121 (2025).
[68] V. Weisskopf and E. Wigner, Berechnung der Natürlichen Linienbreite auf Grund der Diracschen Lichttheorie, Z. Phys. **63**, 54 (1930).
[69] G. S. Agarwal, *Quantum Optics*, 1st ed. (Cambridge University Press, Cambridge, England, 2013).
[70] C. J. Campbell, A. G. Radnaev, A. Kuzmich, V. A. Dzuba, V. V. Flambaum, and A. Derevianko, Single-ion nuclear clock for metrology at the 19th decimal place, Phys. Rev. Lett. **108**, 120802 (2012).
[71] J. Tiedau, M. V. Okhapkin, K. Zhang, J. Thielking, G. Zitzer, E. Peik, F. Schaden, T. Pronebner, I. Morawetz, L. T. De Col, F. Schneider, A. Leitner, M. Pressler, G. A. Kazakov, K. Beeks, T. Sikorsky, and T. Schumm, Laser excitation of the Th-229 nucleus, Phys. Rev. Lett. **132**, 182501 (2024).